Eng. Opt., 2002, Vol. 34, pp. 645–669

MULTI-OBJECTIVE OPTIMIZATION OF SKELETAL STRUCTURES UNDER STATIC AND SEISMIC LOADING CONDITIONS

MANOLIS PAPADRAKAKIS*, NIKOS D. LAGAROS and VAGELIS PLEVRIS

Institute of Structural Analysis and Seismic Research, National Technical University of Athens, Zografou Campus, Athens 157-80, Greece

(Received 16 April 2002)

Almost every real world problem involves simultaneous optimization of several incommensurable and often competing objectives which constitutes a multi-objective optimization problem. In multi-objective optimization problems the optimal solution is not unique as in single-objective optimization problems. This paper is concerned with large-scale structural optimization of skeletal structures such as space frames and trusses, under static and/or seismic loading conditions with multiple objectives. Combinatorial optimization methods and in particular algorithms based on evolution strategies are implemented for the solution of this type of problems. In treating seismic loading conditions a number of accelerograms are produced from the elastic design response spectrum of the region. These accelerograms constitute the multiple loading conditions under which the structures are optimally designed. This approach for treating seismic loading is compared with an approximate design approach, based on simplifications adopted by the seismic codes, in the framework of multi-objective optimization.

Keywords: Multi-objective structural optimization; Evolution strategies; Seismic loading

1 INTRODUCTION

In single-objective optimization problems the optimal solution is usually clearly defined since it is the minimum or maximum value of the objective function. This does not hold in real world problems where multiple and conflicting objectives frequently exist. Instead of a single optimal solution, there is usually a set of alternative solutions, generally denoted as the set of Pareto optimal solutions. These solutions are optimal in the wider sense since no other solution in the search space is superior to them when all objectives are considered. In the absence of preference information, none of the corresponding trade-offs can be said to be better than the others. On the other hand, the search space can be very large and complex, which is the usual case of real world problems, hence the implementation of gradient based optimizers for this type of problem becomes even more cumbersome. Thus, efficient optimization strategies are required able to deal with the presence of multiple objectives and the complexity of the search space. Evolutionary Algorithms (EA) have several

* Corresponding author. E-mail: mpapadra@central.ntua.gr

ISSN 0305-215X print; ISSN 1029-0273 online © 2002 Taylor & Francis Ltd
DOI: 10.1080/0305215021000040728

characteristics that are desirable for this kind of problem and most frequently outperform the deterministic optimizers such as gradient based optimization algorithms.

There are some standard methods for dealing with multi-objective optimization problems, such as the linear weighting method, the distance function method and the constraint method [1–3], that have to be combined with the optimization algorithm. The application of EA in multi-objective optimization problems has received considerable attention in the last five years due to this difficulty of conventional optimization techniques, to be extended to multi-objective optimization problems [4]. EA optimizers employ multiple individuals that can search simultaneously for multiple solutions. Implementing some modifications on the operators used by the EA optimizers, the search process can be driven to a family of solutions representing the set of Pareto optimal solutions.

Structural sizing optimization since its early stages of development was mostly single-objective. The aim was to minimize the weight of the structure under certain restrictions imposed by design codes. Optimization of large-scale structures, such as sizing optimization of multi-storey 3D frames and trusses is a computationally intensive task. The optimization problem becomes more intensive when dynamic loading is involved [5]. The feasible design space in structural optimization problems under dynamic constraints is often disconnected or disjoint [6] which cause difficulties for many conventional optimizers. Due to the uncertain nature of the seismic loading, structural designs are often based on design response spectra of the region and on some simplified assumptions of the structural behavior under seismic loading. In the case of a direct consideration of seismic loading the optimization of structural systems requires the solution of the dynamic equations of motion which can be orders of magnitude more computationally intensive than the case of static loading.

The performance of the proposed method for handling optimization problems with multiple objectives is examined in two test examples, one space frame and one space truss. In the case of the space truss only static loading conditions have been considered. In the case of the space frame, both a rigorous approach and a simplified one with respect to the loading condition are implemented and their efficiency is compared in the framework of finding the optimum design of a structure under multiple objectives. In the context of the rigorous approach a number of artificial accelerograms are produced from the design response spectrum of the region for elastic structural response, which constitutes the multiple loading conditions under which the structures are optimally designed. The elastic design response spectrum can be seen as an envelope of response spectra, for a specific damping ratio, of different earthquakes most likely to occur in the region. This approach is compared with the approximate one based on simplifications adopted by the seismic codes. The Pareto sets obtained for a characteristic problem indicate differences between the two Pareto sets obtained by the rigorous approach and the simplified one.

2 SINGLE-OBJECTIVE STRUCTURAL OPTIMIZATION

In sizing optimization problems the aim is to minimize a single objective function, usually the weight of the structure, under certain behavioral constraints on stress and displacements. The design variables are most frequently chosen to be dimensions of the cross-sectional areas of the members of the structure. Due to fabrication limitations the design variables are not continuous but discrete since cross-sections belong to a certain set. A discrete structural optimization problem can be formulated in the following form

$$\begin{array}{lll} \min & f(\mathbf{s}) & \\ \text{subject to} & g_j(\mathbf{s}) \leq 0 & j = 1, \ldots, k \\ & s_i \in R^d & i = 1, \ldots, n \end{array} \tag{1}$$

where R^d is a given set of discrete values and the design variables $s_i (i = 1, \ldots, n)$ can take values only from this set.

In the optimal design of frames the constraints are the member stresses and nodal displacements or inter-storey drifts. For rigid frames with I-shapes, the stress constraints, under allowable stress design requirements specified by Eurocode 3 [7], are expressed by the following formula

$$\frac{N_{sd}}{Af_y/\gamma_{\mathrm{M1}}} + \frac{M_{y,sd}}{W_{pl,y}f_y/\gamma_{\mathrm{M1}}} + \frac{M_{z,sd}}{W_{pl,z}f_y/\gamma_{\mathrm{M1}}} \leq 1.0 \tag{2}$$

where N_{sd}, $M_{sd,y}$, $M_{sd,z}$ are the stress resultants, $W_{pl,y}$, $W_{pl,z}$ are the plastic first moment of inertia, and f_y is the yield stress. The safety factor γ_{M1} is a Eurocode 1 [8] box value usually taken as 1.10.

Space truss structures usually have the topology of single or multi-layered flat or curved grids that can be easily constructed in practice. In the optimal design of trusses the constraints are the member stresses, nodal displacements, or frequencies. The stress constraints can be written as $|\sigma| \leq |\sigma_a|$, where σ is the maximum axial stress in each element group for all loading cases, $\sigma_a = f_y/\gamma_{\mathrm{M1}}$ is the allowable axial stress. Similarly, the displacement constraints can be written as $|d| \leq d_a$, where d_a is the limiting value of the displacement at a certain node, or the maximum nodal displacement.

Euler buckling is also considered as a stress-type constraint in truss structures. This is enforced when the magnitude of a member's compressive stress is greater than a critical stress which usually is taken as the first buckling mode of a pin-connected member:

$$\sigma_b = \frac{P_b}{A} = -\frac{1}{A}\left(\frac{\pi^2 EI}{L^2}\right) \tag{3}$$

where P_b is the computed compressive axial force, I is the moment of inertia, L is the member length. Thus, the compressive stress should be less (in absolute values) than the critical Euler buckling stress $|\sigma| \leq |\sigma_b|$.

3 MULTI-OBJECTIVE STRUCTURAL OPTIMIZATION

In practical applications of structural optimization of 3D frames and trusses the material weight rarely gives a representative measure of the performance of the structure. In fact, several conflicting and incommensurable criteria usually exist in real-life design problems, that have to be dealt with simultaneously. This situation forces the designer to look for a good compromise design between the conflicting requirements. These kinds of problems are called optimization problems with many objectives. The consideration of multi-objective optimization in its present sense originated towards the end of the 19th century when Pareto presented the optimality concept in economic problems with several competing criteria [9]. Since then, although many techniques have been developed in order to deal with multi-objective optimization problems the corresponding applications were confined strictly to mathematical functions. The first applications in the field of structural optimization with multiple objectives appeared at the end of the 1970s. However only a few Pareto structural optimization problems have been considered and those were restricted to multi-objective optimization problems with static loading conditions [10–16].

3.1 Criteria and Conflict

The designer looking for the optimum design of a structure is faced with the question of selecting the most suitable criteria for measuring the economy, the strength, the serviceability or any other factor that affects the performance of a structure. Any quantity that has a direct influence on the performance of the structure can be considered as a criterion. On the other hand, those quantities that must satisfy some imposed requirements are not criteria but they can be treated as constraints. Most of the structural optimization problems are treated with one single-objective usually the weight of the structure, subjected to some strength constraints. These constraints are set as equality or inequality constraints using some upper and lower limits. When there is a difficulty in selecting these limits, then these parameters are better treated as criteria.

One important basic property in the multicriterion formulation is the conflict that may or may not exist between the criteria. Only those quantities that are competing should be treated as independent criteria whereas the others can be combined into a single criterion to represent the whole group. The local conflict between two criteria can be defined as follows: The functions f_i and f_j are called locally collinear with no conflict at point $\mathbf{s}$ if there is $c > 0$ such that $\nabla f_i(\mathbf{s}) = c\nabla f_j(\mathbf{s})$. Otherwise, the functions are called locally conflicting at $\mathbf{s}$. According to this definition any two criteria are locally conflicting at a point of the design space if their maximum improvement is achieved in different directions. The global conflict between two criteria can be defined as follows: The functions f_i and f_j are called globally conflicting in the feasible region $\mathcal{F}$ of the design space when the two optimization problems $\min_{\mathbf{s}\in\mathcal{F}} f_i(\mathbf{s})$ and $\min_{\mathbf{s}\in\mathcal{F}} f_j(\mathbf{s})$ have different optimal solutions.

3.2 Formulation of a Multiple Objective Optimization Problem

In formulating an optimization problem the choice of the design variables, criteria and constraints represents undoubtedly the most important decision made by the engineer. In general the mathematical formulation of a multi-objective problem includes a set of n design variables, a set of m objective functions and a set of k constraint functions and can be defined as follows:

$$\begin{array}{lll} \min_{\mathbf{s}\in\mathcal{F}} & [f_1(\mathbf{s}), f_2(\mathbf{s}), \ldots, f_m(\mathbf{s})]^{\mathrm{T}} & \\ \text{subject to} & g_j(\mathbf{s}) \le 0 & j = 1, \ldots, k \\ & s_i \in R^d & i = 1, \ldots, n \end{array} \tag{4}$$

where the vector $\mathbf{s} = [s_1 s_2 \cdots s_n]^{\mathrm{T}}$ represents a design variable vector and $\mathcal{F}$ is the feasible set in design space R^n. It is defined as the set of design variables that satisfy the constraint functions $\mathrm{g}(\mathbf{s})$ in the form:

$$\mathcal{F} = \{\mathbf{s} \in R^n | \mathrm{g}(\mathbf{s}) \le 0\} \tag{5}$$

Usually there exists no unique point which would give an optimum for all m criteria simultaneously. Thus the common optimality condition used in single-objective optimization must be replaced by a new concept, the so-called Pareto optimum: A design vector $\mathbf{s}^* \in \mathcal{F}$ is Pareto optimal for the problem of Eq. (5) if and only if there exists no other design vector $\mathbf{s} \in \mathcal{F}$ such that

$$f_i(\mathbf{s}) \le f_i(\mathbf{s}^*) \quad \text{for } i = 1, 2, \ldots, m \tag{6}$$

with $f_j(\mathbf{s}) < f_j(\mathbf{s}^*)$ for at least one objective j.

The solutions of optimization problems with multiple objectives constitute the set of the Pareto optimum solutions. The problem of Eq. (5) can be regarded as being solved when the set of Pareto optimal solutions has been determined. In practical applications, however, the designer seeks for a unique final solution. Thus a compromise should be made among the available Pareto optimal solutions.

3.3 Solving the Multi-objective Optimization Problem

Standard methods for generating the Pareto optimal set combine the objectives into a single, parameterized objective function. Basically, this procedure is independent of the incorporated optimization algorithm. Three previously used methods in the literature are briefly discussed and are compared in this study with the proposed modified ES in terms of computational time and efficiency for treating multi-objective optimization problems.

3.3.1 Linear Weighting Method

The first method, called the linear weighting method [3], combines all the objectives into a single scalar parameterized objective function by using weighting coefficients. If w_i, $i = 1, 2, \ldots, m$ are the weighting coefficients the problem of Eq. (5) can be written as follows:

$$\min_{\mathbf{s}\in\mathcal{F}} \sum_{i=1}^{m} w_i f_i(\mathbf{s}) \tag{7}$$

With no loss of generality the following normalization of the weighting coefficients is employed

$$\sum_{i=1}^{m} w_i = 1 \tag{8}$$

By varying these weights it is now possible to generate the set of Pareto optimal solutions for the problem of Eq. (5). The values of the weighting coefficients are adjusted according to the importance of each criterion. Every combination of those weighting coefficients corresponds to a single Pareto optimal solution, thus by performing a set of optimization processes using different weighting coefficients it is possible to generate the full set of Pareto optimal solutions.

In real world problems different units correspond to different objectives leading to variations of some orders of magnitude between the values of the objectives. It is therefore advisable that the objectives should be normalized according the following expression:

$$\tilde{f}_i(\mathbf{s}) = \frac{f_i(\mathbf{s}) - f_{i\min}}{f_{i\max} - f_{i\min}} \tag{9}$$

where the normalized objectives $\tilde{f}_i(\mathbf{s}) \in [0, 1]$, $i = 1, 2, \ldots, m$, share the same design space with the non-normalized ones, while $f_{i\min}$ and $f_{i\max}$ are the minimum and maximum values of the objective function i.

3.3.2 Distance Function Method

The distance methods [1] are based on the minimization of the distance between the set of the objective function values and some chosen reference points belonging to the so-called

criterion space. Criterion space is defined as the set of the objective function values that correspond to design vectors of the feasible domain. The resulting scalar problem is:

$$\min_{\mathbf{s}\in\mathcal{F}} d_p(\mathbf{s}) \tag{10}$$

where the distance function can be written as follows:

$$d_p(\mathbf{s}) = \left\{ \sum_{i=1}^{m} w_i [f_i(\mathbf{s}) - z_i]^p \right\}^{1/p} \tag{11}$$

and p is an integer number.

This technique has been implemented in structural optimization in Ref. [17]. The reference point $z^{id} \in R^m$ that is selected by the designer is also called the ideal or utopian point. A reference point that is frequently used is the following:

$$z^{id} = [\, f_{1\,\min}\, f_{2\,\min} \cdots f_{m\,\min}]^{\mathrm{T}} \tag{12}$$

where $f_{i\,\min}$ is the optimum solution of the single-objective optimization problem where the ith objective function is treated as the unique objective. The normalization function, Eq. (8), for the weighting factors w_i is also used. In the case that $p = \infty$ Eq. (10) is transformed to the minimax problem:

$$\min_{\mathbf{s}\in\mathcal{F}} \max_i [w_i f_i(\mathbf{s})], \quad i = 1, 2, \ldots, m \tag{13}$$

In the case of $p = 1$ the formulation of the distance method is equivalent to the linear method when the reference point used is the zero $\hat{z} = 0$, while the case of $p = 2$ the method is called the weighted quadratic method.

3.3.3 Constraint Method

According to this method the original multicriterion problem is replaced by a scalar problem where one criterion f_k is chosen as the objective function and all the other criteria are removed into the constraints [2]. By introducing parameters ε_i into these new constraints an additional feasible set is obtained:

$$\mathcal{F}_k(\varepsilon_i) = \{\mathbf{s} \in R^n | f_i(\mathbf{s}) \le \varepsilon_i, \quad i = 1, 2, \ldots, m \text{ with } i \ne k\} \tag{14}$$

If the resulting feasible set is denoted by $\bar{\mathcal{F}}_k = \mathcal{F} \cap \mathcal{F}_k$ the parameterized scalar problem can be expressed as:

$$\min_{\mathbf{s}\in\bar{\mathcal{F}}_k} f_k(\mathbf{s}) \tag{15}$$

The constraint method gives the opportunity to obtain the full domain of optimum solutions, in the horizontal or vertical direction using one criterion as objective function and the other as constraint.

3.3.4 Modified Evolution Strategies for Multi-objective Optimization

The three above-mentioned methods for multi-objective optimization have been used in the past with mathematical programming optimization algorithms where at each optimization

step one design point was examined as an optimum design candidate. in order to locate the set of Pareto optimum solutions a family of optimization runs have to be executed. On the other hand, evolutionary algorithms work simultaneously with a population of design points, instead of a single design point, which constitute a population of optimum design candidates in the space of design variables. Due to this characteristic, evolutionary algorithms have a great potential in finding multiple optima in a single optimization run, which is very useful in Pareto optimization problems. Since the early 1990s a number of researchers have suggested the use of evolutionary algorithms in multi-objective optimization problems [4, 18–21].

In this study the method of Evolution Strategies (ES) is applied for the first time in structural multi-objective optimization problems. To this purpose some modifications have to be made in the random operators in order to guide the convergence to a population that represent the set of Pareto optimal solutions. These changes refer to (i) the selection of the parent population at each generation that has to be modified in order to guide the search procedure towards the set of Pareto optimum solutions, and (ii) the prevention from convergence to a single design point and preservation of diversity of the population in every generation step. The first demand is possible to be fulfilled using random selection of the objective according to which the individual will be chosen for reproduction [18]. In order to preserve diversity in the population and fulfil the second requirement, fitness sharing is implemented.

The idea behind sharing is to degrade those individuals that are represented by higher percentages in the population. the expression for the modified objectives after sharing is given by:

$$f_i'(\mathbf{s}) = \frac{f_i(\mathbf{s})}{\sum_h \mathrm{sh}(d(\mathbf{s}, h))} \tag{16}$$

where the sharing function used in the current study is the following

$$\mathrm{sh}(d(\mathbf{s}, h)) = \begin{cases} 1 - \left(\dfrac{d(\mathbf{s}, h)}{\sigma_{\mathrm{share}}}\right)^{\alpha} & \text{if } d(\mathbf{s}, h) < \sigma_{\mathrm{share}} \\ 0 & \text{otherwise} \end{cases} \tag{17}$$

and the distance function used is in the objective space takes the form

$$d(\mathbf{s}, h) = \|f(\mathbf{s}) - f(h)\| \tag{18}$$

4 STRUCTURAL DESIGN UNDER DYNAMIC LOADING

The equations of equilibrium for a finite element system in motion for the ith design vector can be written in the usual form

$$\mathbf{M}(\mathbf{s}_i)\ddot{\mathbf{u}}_t + \mathbf{C}(\mathbf{s}_i)\dot{\mathbf{u}}_t + \mathbf{K}(\mathbf{s}_i)\mathbf{u}_t = \mathbf{R}_t \tag{19}$$

where $\mathbf{M}(\mathbf{s}_i)$, $\mathbf{C}(\mathbf{s}_i)$, and $\mathbf{K}(\mathbf{s}_i)$ are the mass, damping and stiffness matrices for the ith design vector $\mathbf{s}_i$; $\mathbf{R}_t$ is the external load vector, while $\mathbf{u}$, $\dot{\mathbf{u}}$ and $\ddot{\mathbf{u}}$ are the displacement, velocity, and acceleration vectors of the finite element assemblage, respectively. The solution methods of direct integration of equations of motion and of response spectrum modal analysis, which is based on the mode superposition approach, will be considered in the following paragraphs.

The Newmark integration scheme is adopted in the present study to perform the direct time integration of the equations of motion where the equilibrium equations (19) are discretized in time as follows

$$\mathbf{M}(\mathbf{s}_i)\ddot{\mathbf{u}}_{t+\Delta t} + \mathbf{C}(\mathbf{s}_i)\dot{\mathbf{u}}_{t+\Delta t} + \mathbf{K}(\mathbf{s}_i)\mathbf{u}_{t+\Delta t} = \mathbf{R}_{t+\Delta t} \tag{20}$$

and the variation of velocity and displacement are given by

$$\dot{\mathbf{u}}_{t+\Delta t} = \dot{\mathbf{u}}_t + [(1-\delta)\ddot{\mathbf{u}}_t + \delta\ddot{\mathbf{u}}_{t+\Delta t}]\Delta t \tag{21}$$

$$\mathbf{u}_{t+\Delta t} = \mathbf{u}_t + \dot{\mathbf{u}}_t\Delta t + \left[\left(\frac{1}{2} - \alpha\right)\ddot{\mathbf{u}}_t + \alpha\ddot{\mathbf{u}}_{t+\Delta t}\right]\Delta t^2 \tag{22}$$

where α and δ are parameters that can be determined to obtain integration accuracy and stability. Solving for $\ddot{\mathbf{u}}_{t+\Delta t}$ in terms of $\mathbf{u}_{t+\Delta t}$ from Eq. (22) and substituting for $\ddot{\mathbf{u}}_{t+\Delta t}$ in Eq. (21) yields equations for $\ddot{\mathbf{u}}_{t+\Delta t}$ and $\dot{\mathbf{u}}_{t+\Delta t}$ in terms of the unknown displacements $\mathbf{u}_{t+\Delta t}$ only. These two relations for $\ddot{\mathbf{u}}_{t+\Delta t}$ and $\dot{\mathbf{u}}_{t+\Delta t}$ are then substituted into Eq. (20) to solve for $\mathbf{u}_{t+\Delta t}$. As a result of this substitution the following well-known equilibrium equation is obtained at each time step

$$\mathbf{K}_{\text{eff}}(\mathbf{s}_i)\mathbf{u}_{t+\Delta t} = \mathbf{R}^{\text{eff}}_{t+\Delta t} \tag{23}$$

4.1 Creation of Artificial Accelerograms

The selection of the proper external loading $\mathbf{R}_t$ to perform structural analyses under seismic loading conditions for design purposes is not an easy task due to the uncertainties involved in the seismic loading. For this reason a rigorous treatment of the seismic loading is to assume that the structure is subjected to a set of real and/or artificial earthquakes that are likely to occur in the region where the structure is located. These artificial seismic excitations are produced as a series of artificial accelerograms compatible with the elastic design response spectrum of the region.

In this work the implementation published by Taylor [22] for the generation of statistically independent artificial acceleration time histories is adopted. This method is based on the fact that any periodic function can be expanded into a series of sinusoidal waves

$$x(t) = \sum_k A_k \sin(\omega_k t + \varphi_k) \tag{24}$$

where A_k is the amplitude, ω_k is the cyclic frequency and φ_k is the phase angle of the kth contributing sinusoid. By fixing an array of amplitudes and then generating different arrays of phase angles, different motions can be generated which are similar in general appearance but different in the "details". The computer uses a random number generator subroutine to produce strings of phase angles with a uniform distribution in the range between 0 and 2π. The amplitudes A_k are related to the spectral density function in the following way

$$G(\omega_k)\Delta\omega = \frac{A_k^2}{2} \tag{25}$$

where $G(\omega_k)\Delta\omega$ may be interpreted as the contribution to the total power of the motion from the sinusoid with frequency ω_k. The power of the motion produced by Eq. (24) does not vary

with time. To simulate the transient character of real earthquakes, the steady-state motions are multiplied by a deterministic envelope function $I(t)$

$$Z(t) = I(t) \sum_k A_k \sin(\omega_k t + \varphi_k) \tag{26}$$

The resulting motion is stationary in frequency content with peak acceleration close to the target peak acceleration. In this study a trapezoidal intensity envelope function is adopted. The generated peak acceleration is artificially modified to match the target peak acceleration, which corresponds to the chosen elastic design response spectrum. An iterative procedure is then implemented to smooth the calculated spectrum and improve the matching [22].

The elastic design response spectrum considered in the current study is depicted in Figure 1 for damping ratio $\xi = 2.5\%$. Five artificial uncorrelated accelerograms, produced by the previously discussed procedure and shown in Figure 2, have been used as the input seismic excitation for the numerical tests. The corresponding response spectrum of the first artificial accelerogram is also depicted in Figure 1.

4.2 Response Spectrum Modal Analysis

The response spectrum modal analysis is based on a simplification of the mode superposition approach with the aim to avoid the time history analyses which are required by both the direct integration and mode superposition approaches. In the case of the response spectrum modal analysis Eq. (4) is modified according to the modal superposition approach, for the ith design vector, in the following form

$$\bar{\mathbf{M}}(\mathbf{s}_i)\ddot{\mathbf{u}}_t + \bar{\mathbf{C}}(\mathbf{s}_i)\dot{\mathbf{u}}_t + \bar{\mathbf{K}}(\mathbf{s}_i)\mathbf{u}_t = \bar{\mathbf{R}}_t \tag{27}$$

where

$$\bar{\mathbf{M}}(\mathbf{s}_i) = \mathbf{\Phi}_i^{\mathrm{T}}\mathbf{M}_i\mathbf{\Phi}_i \tag{28}$$

$$\bar{\mathbf{C}}(\mathbf{s}_i) = \mathbf{\Phi}_i^{\mathrm{T}}\mathbf{C}_i\mathbf{\Phi}_i \tag{29}$$

$$\bar{\mathbf{K}}(\mathbf{s}_i) = \mathbf{\Phi}_i^{\mathrm{T}}\mathbf{K}_i\mathbf{\Phi}_i \tag{30}$$

$$\bar{\mathbf{R}}_t = \mathbf{\Phi}_i^{\mathrm{T}}\mathbf{R}_t \tag{31}$$

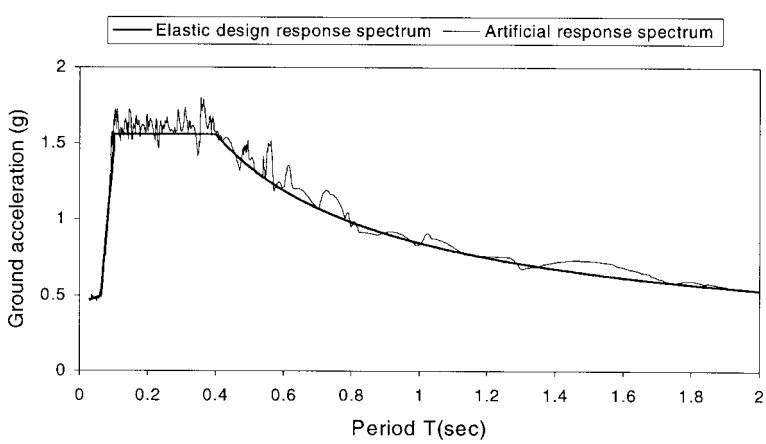

FIGURE 1 Elastic design response spectrum of the region and response spectrum of the first artificial accelerogram ($\xi = 2.5\%$).

are the generalized values of the corresponding matrices and the loading vector, while $\mathbf{\Phi}_i$ is an eigenmode shape matrix to be defined later. For simplicity $\mathbf{M}(\mathbf{s}_i)$, $\mathbf{C}(\mathbf{s}_i)$, $\mathbf{K}(\mathbf{s}_i)$ are denoted by $\mathbf{M}_i$, $\mathbf{C}_i$, $\mathbf{K}_i$, respectively. These matrices correspond to the design, which is defined by the ith vector of the design parameters. According to the modal superposition approach the system of N simultaneous differential equations is transformed to a set of N independent normal-coordinate equations.

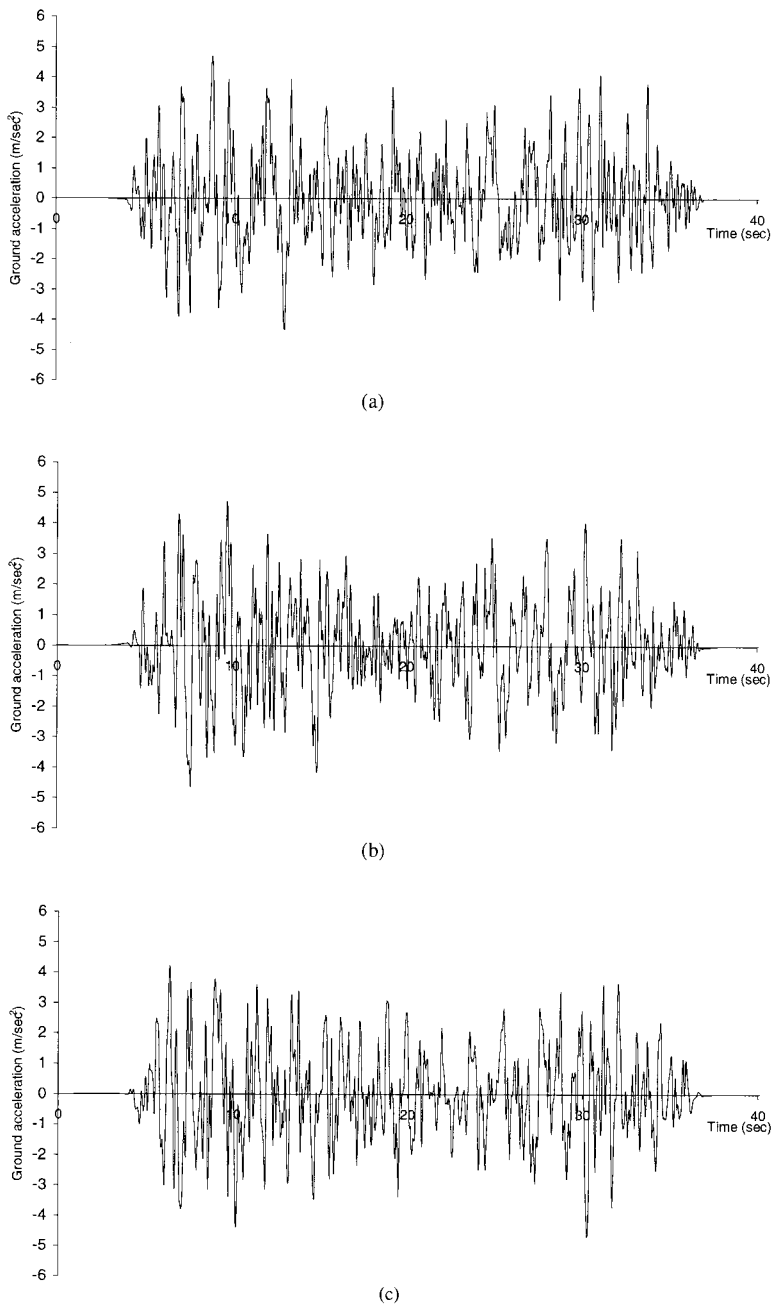

FIGURE 2 The five artificial accelerograms.

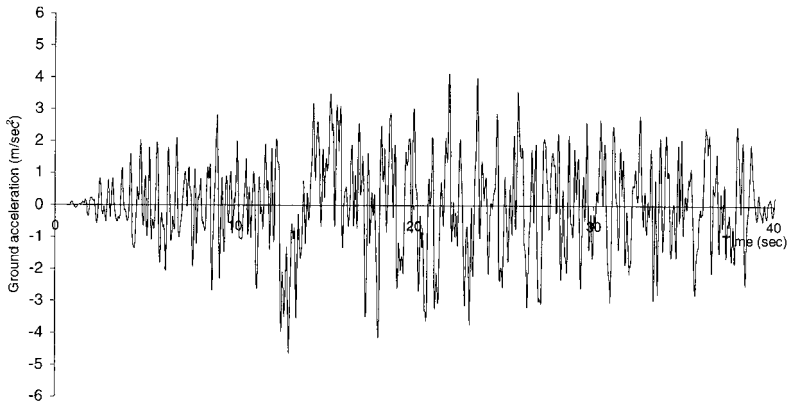

(d)

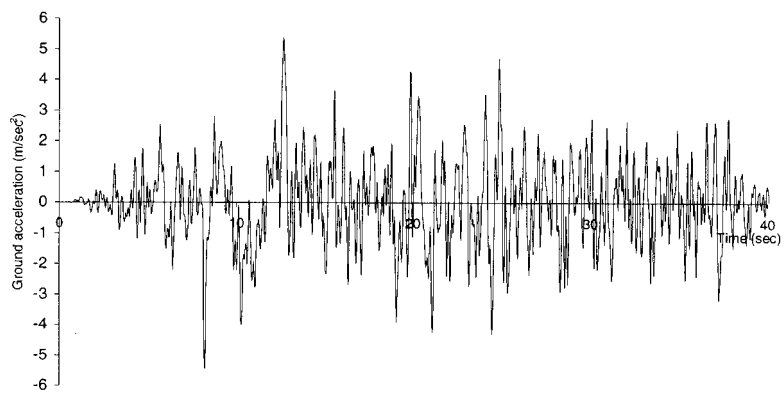

(e)

FIGURE 2 *(Continued)*.

In the response spectrum modal analysis a number of different formulas have been proposed to obtain reasonable estimates of the maximum response based on the spectral values without performing time history analyses for a considerable number of transformed dynamic equations. The simplest and most popular of these is the square root of the sum of the squares (SRSS) of the modal responses. According to this estimate the maximum total displacement is approximated by

$$u_{\max} = \sqrt{\mathbf{u}_{1,\max}^2 + \mathbf{u}_{2,\max}^2 + \cdots + \mathbf{u}_{N,\max}^2} \tag{32}$$

where $\mathbf{u}_{j,\max}$ corresponds to the maximum displacement calculated from the jth transformed dynamic equations over the complete time period. The use of the Eq. (32) permits this type of "dynamic" analysis by knowing only the maximum modal coordinates $u_{j,\max}$.

The following steps summarize the response spectrum modal analysis adopted in this study and by a number of seismic codes around the world:

1. Calculate a number $m' < N$ of eigenfrequencies and the corresponding eigenmode shape matrices, which are classified in the following order $(\omega_i^1, \omega_i^2, \ldots, \omega_i^{m'})$, $\mathbf{\Phi}_i = [\boldsymbol{\phi}_i^1, \boldsymbol{\phi}_i^2, \ldots, \boldsymbol{\phi}_i^{m'}]$, respectively, where ω_i^j, $\boldsymbol{\phi}_i^j$ are the jth eigenfrequency–eigenmode

corresponding to the ith design vector. m′ is a user specified number, based on experience or on previous test analyses, which has to satisfy the requirement of Step 6.

2. Calculate the generalized masses:

$$\bar{m}_i^j = \boldsymbol{\phi}_i^{j^{\mathrm{T}}} \mathbf{M}_i \boldsymbol{\phi}_i^j \tag{33}$$

3. Calculate the coefficients L_i^j:

$$L_i^j = \boldsymbol{\phi}_i^{j^{\mathrm{T}}} \mathbf{M}_i \mathbf{r} \tag{34}$$

where $\mathbf{r}$ is the influence vector, which represents the displacements of the masses resulting from static application of a unit ground displacement.

4. Calculate the modal participation factor Γ_i^j:

$$\Gamma_i^j = \frac{L_i^j}{\bar{m}_i^j} \tag{35}$$

5. Calculate the effective modal mass for each design vector and for each eigenmode:

$$m_{\mathrm{eff},i}^j = \frac{L_i^{j^2}}{\bar{m}_i^j} \tag{36}$$

6. Calculate a number $m < m'$ of the important eigenmodes. According to Eurocode the minimum number of eigenmodes that have to be taken into consideration is defined by the following assumption: The sum of the effective eigenmasses must not be less than the 90% of the total vibrating mass m_{tot} of the system. Thus the first m eigenmodes that satisfy the equation

$$\sum_{j=1}^{m} m_{\mathrm{eff},i}^j \geq 0.90 m_{\mathrm{tot}} \tag{37}$$

are taken into consideration.

7. Calculate the values of the spectral acceleration $R_d(T_j)$ that correspond to each eigenperiod T_j of the m important modes from the response spectrum of the region.
8. Calculate the modal displacements according to equation

$$(\mathrm{SD})_j = \frac{R_d(T_j)}{\omega_j^2} = \frac{R_d(T_j) \cdot T_j^2}{4\pi^2}, \quad j = 1, \ldots, m \tag{38}$$

9. Calculate the maximum modal displacements for

$$\mathbf{u}_{j,\max} = \Gamma_i^j \cdot \boldsymbol{\phi}_i^j \cdot (\mathrm{SD})_j, \quad j = 1, \ldots, m \tag{39}$$

10. The total maximum displacement is calculated by superimposing the maximum modal displacements according to Eq. (32).

5 SOLUTION OF THE OPTIMIZATION PROBLEM

Evolutionary Computation (EC) encompasses methods of simulating evolution on computing systems. Evolutionary Algorithms (EA) belong to EC and represent the probabilistic category of optimization methods. The first attempt in the field of evolutionary computation was focused on building a computer program that would simulate the process of evolution in nature. Evolutionary algorithms have been found to be capable of producing very powerful and robust search mechanisms although the similarity between these algorithms and natural evolution is based on a crude imitation of biological reality. The resulting evolutionary algorithms are based on a population of individuals, which are subjected to processes of mutation, recombination/crossover and selection.

In structural optimization problems, where the objective function and the constraints are highly non-linear functions of the design variables, the computational effort spent in gradient calculations required by the mathematical programming algorithms is usually large. In two studies [23, 24] it was found that probabilistic search algorithms are computationally efficient even if greater number of optimization cycles is needed to reach the optimum. These cycles are computationally less expensive than in the case of mathematical programming algorithms since they do not need gradient evaluation. Furthermore, probabilistic methodologies were found to be more robust in finding the global optimum, due to their random search, whereas mathematical programming algorithms may be trapped in local optima.

5.1 ES for Discrete Optimization Problems

Evolution strategies (ES) methodology represents a probabilistic search and optimization algorithm based on principles of organic evolution and was proposed for parameter optimization problems in the 1970s [25]. The multi-membered ES adopted in the current study, based on the discrete formulation [26], uses three operators: recombination, mutation and selection operators that can be included in the algorithm as follows:

Step 1 (recombination and mutation) The population of μ parents at the gth generation produces λ offsprings. The genotype of any descendant differs only slightly from that of its parents. For every offspring vector a temporary parent vector $\tilde{\mathbf{s}} = [\tilde{s}_1, \tilde{s}_2, \ldots, \tilde{s}_n]^{\mathrm{T}}$ is first built by means of recombination. For discrete problems the following recombination cases can be used

$$\tilde{s}_i = \begin{cases} s_{\alpha,i} \text{ or } s_{b,i} \text{ randomly} & \text{(A)} \\ s_{m,i} \text{ or } s_{b,i} \text{ randomly} & \text{(B)} \\ s_{bj,i} & \text{(C)} \\ s_{\alpha,i} \text{ or } s_{bj,i} \text{ randomly} & \text{(D)} \\ s_{m,i} \text{ or } s_{bj,i} \text{ randomly} & \text{(E)} \end{cases} \tag{40}$$

$\tilde{s}_i$ is the ith component of the temporary parent vector $\tilde{\mathbf{s}}$, $s_{\alpha,i}$ and $s_{b,i}$ are the ith components of the vectors $\mathbf{s}_a$ and $\mathbf{s}_b$ which are two parent vectors randomly chosen from the population. The vector $\mathbf{s}_m$ is not randomly chosen but is the best of the μ parent vectors in the current generation. In case (C) of Eq. (40), $\tilde{s}_i = s_{bj,i}$ means that the ith component of $\tilde{\mathbf{s}}$ is chosen randomly from the ith components of all μ parent vectors. From the temporary parent $\tilde{\mathbf{s}}$ an offspring can be created following the mutation operator.

The mutation operator generates an offspring $\mathbf{s}_o$, from the temporary parent vectors, whose genotype is slightly different from the parental one:

$$\mathbf{s}_o = \tilde{\mathbf{s}} + \mathbf{z} \tag{41}$$

where $\mathbf{z} = [z_1, z_2, \ldots, z_n]^{\mathrm{T}}$ is a random vector. The random vector $\mathbf{z}$ is properly generated in order to force the offspring vector to move to another set of discrete values. The fact that the difference between any two adjacent values can be relatively large is contrary to the requirement that the variance σ_i^2 should be small. For this reason it is suggested that not all the components of a parent vector, but only a few of them (*e.g.* ℓ), should be randomly changed in every generation. This means that $n - \ell$ components of the randomly changed vector $\mathbf{z}^{(g)}$ will have zero value. In other words, the terms of vector $\mathbf{z}^{(g)}$ are derived from

$$z_i^{(g)} = \begin{cases} (\kappa + 1)\delta s_i & \text{for } \ell \text{ randomly chosen components} \\ 0 & \text{for } n - \ell \text{ other components} \end{cases} \tag{42}$$

where δs_i is the difference between two adjacent values in the discrete set and κ is a random integer number, which follows the Poisson distribution

$$p(\kappa) = \frac{(\gamma)^{\kappa}}{\gamma!} e^{-\gamma} \tag{43}$$

γ is the standard deviation as well as the mean value of the random number κ.

Step 2 (selection) There are two different types of the multi-membered ES:

$(\mu + \lambda)$-ES: The best μ individuals are selected from a temporary population of $(\mu + \lambda)$ individuals to form the parents of the next generation.

(μ, λ)-ES: The μ individuals produce λ offsprings $(\mu \leq \lambda)$ and the selection process defines a new population of μ individuals from the set of λ offsprings only.

In order to implement ES in Pareto optimization problems the selection operator is based on a randomly chosen objective. For discrete optimization the procedure terminates when one of the following termination criteria is satisfied: (i) when the best value of the objective function in the last $4n\mu/\lambda$ generations remains unchanged, (ii) when the mean value of the objective values from all parent vectors in the last $2n\mu/\lambda$ generations has not been improved by less than a given value ε_b $(=0.0001)$, (iii) when the relative difference between the best objective function value and the mean value of the objective function values from all parent vectors in the current generation is less than a given value ε_c $(=0.0001)$, (iv) when the ratio μ_b/μ has reached a given value ε_d $(=0.5$ to $0.8)$ where μ_b is the number of the parent vectors in the current generation with the best objective function value.

5.2 ES in Multi-objective Structural Optimization Problems

The application of evolutionary algorithms in multi-objective optimization problems has attracted the interest of a number of researchers in the last five years due to the difficulty of conventional optimization techniques, such as gradient based methods, to be extended to multi-objective optimization problems. EA, however, have been recognized to be more appropriate to multi-objective optimization problems since early in their development [1]. Multiple individuals can search for multiple solutions simultaneously, taking advantage of any similarities available in the family of possible solutions to the problem.

In the first implementation where the standard methods are used, the optimization procedure, in order to generate a set of Pareto optimal solutions, initiates with a set of parent design vectors needed by the ES optimizer and a set of weighting coefficients for the combination of all objectives into a single scalar parameterized objective function. These

weighting coefficients are not set by the designer but are systematically varied by the optimizer after a Pareto optimal solution has been achieved. There is an outer loop which systematically varies the parameters of the parameterized objective function, and is called the decision making loop. The inner loop is the classical ES process, starting with a set of parent vectors. If any of these parent vectors gives an infeasible design then this parent vector is modified until it becomes feasible. Subsequently, the offsprings are generated and checked if they are in the feasible region. According to the $(\mu + \lambda)$ selection scheme, in every generation the values of the objective function of the parent and the offspring vectors are compared and the worst vectors are rejected, while the remaining ones are considered to be the parent vectors of the new generation. On the other hand, according to the (μ, λ) selection scheme only the offspring vectors of each generation are used to produce the new generation. This procedure is repeated until the chosen termination criterion is satisfied. The number of parents and offsprings involved affects the computational efficiency of the multi-membered ES discussed in this work. It has been observed that when the values of μ and λ are equal to the number of the design variables better results are produced.

Two ES algorithms for multi-objective structural optimization applications under seismic loading are compared and tested in the subsequent section:

(i) The ES algorithm combined with the standard methods which can be stated as follows:
Outer loop – Decision making loop
Set the parameters w_i of the parameterized objective function
Inner loop – ES loop

1. *Selection step*: selection of $\mathbf{s}_i$ $(i = 1, 2, \ldots, \mu)$ parent vectors of the design variables
2. *Analysis step*: solve $\mathbf{M}(\mathbf{s}_i)\ddot{\mathbf{u}} + \mathbf{C}(\mathbf{s}_i)\dot{\mathbf{u}} + \mathbf{K}(\mathbf{s}_i)\mathbf{u} = \mathbf{R}(t)$ $(i = 1, 2, \ldots, \mu)$
3. *Evaluation of parameterized objective function*
4. *Constraints check*: all parent vectors become feasible
5. *Offspring generation*: generate $s_j, (j = 1, 2, \ldots, \lambda)$ offspring vectors of the design variables
6. *Analysis step*: solve $\mathbf{M}(\mathbf{s}_j)\ddot{\mathbf{u}} + \mathbf{C}(\mathbf{s}_j)\dot{\mathbf{u}} + \mathbf{K}(\mathbf{s}_j)\mathbf{u} = \mathbf{R}(t)$ $(j = 1, 2, \ldots, \lambda)$
7. *Evaluation of the parameterized objective function*
8. *Constraints check*: if satisfied continue, else change s_j and go to Step 5
9. *Selection step*: selection of the next generation parents according to $(\mu + \lambda)$ or (μ, λ) selection schemes
10. *Convergence check*: If satisfied stop, else go to step 5

End of Inner loop
End of Outer loop

(ii) The modified ES algorithm (ESMO) as described in Section 3.3.4 which can be stated as follows:

1. *Selection step*: selection of $\mathbf{s}_i$ $(i = 1, 2, \ldots, \mu)$ parent vectors of the design variables
2. *Analysis step*: solve $\mathbf{M}(\mathbf{s}_i)\ddot{\mathbf{u}} + \mathbf{C}(\mathbf{s}_i)\dot{\mathbf{u}} + \mathbf{K}(\mathbf{s}_i)\mathbf{u} = \mathbf{R}(t)$ $(i = 1, 2, \ldots, \mu)$
3. *Evaluation of the objective functions*
4. *Constraints check*: all parent vectors become feasible
5. *Offspring generation*: generate $s_j, (j = 1, 2, \ldots, \lambda)$ offspring vectors of the design variables
6. *Analysis step*: solve $\mathbf{M}(\mathbf{s}_j)\ddot{\mathbf{u}} + \mathbf{C}(\mathbf{s}_j)\dot{\mathbf{u}} + \mathbf{K}(\mathbf{s}_j)\mathbf{u} = \mathbf{R}(t)$ $(j = 1, 2, \ldots, \lambda)$
7. *Evaluation of the objective functions*
8. *Constraints check*: if satisfied continue, else change $\mathbf{s}_j$ and go to Step 5

9. *Selection step*: random selection of the potential objective for the each individual and selection of the next generation parents according to $(\mu + \lambda)$ or (μ, λ) selection schemes
10. *Fitness sharing*
11. *Convergence check*: If satisfied stop, else go to Step 5

6 NUMERICAL RESULTS

The performance of the multi-objective optimization methods discussed in this paper is investigated in two benchmark test examples: A six storey space frame and a multi-layered space truss. The following abbreviations are used in this section: *DTI* refers to the Newmark Direct Time Integration method. *RSMA* to the Response Spectrum Modal Analysis. *LWM* refers to the Linear Weighting Method, *DFM* to the Distance Function Method and *CM* to the Constraint Method for treating multi-objective optimization problems. Finally *ESMO* refers to the proposed Evolution Strategies for treating Multi-objective Optimization problems.

6.1 Six Storey Space Frame

The objective functions considered for this problem are the weight of the structure, the maximum displacement and the first eigenperiod. The first two objective functions have to be minimized while the third one has to be maximized. Constraints are imposed on the inter-storey drifts and for each element group on the maximum non-dimensional ratio q of Eqs. (2) and (3) under a combination of axial force and bending moments. The test example was run on a Silicon Graphics Power Challenge computer.

The space frame consists of 63 elements with 180 degrees of freedom as shown in Figure 3(a). The length of the beams and the columns are $L_1 = 7.32\,\text{m}$ and $L_2 = 3.66\,\text{m}$, respectively. The structure is loaded with a 19.16 kPa gravity load on all floor levels and a static lateral load of 109 kN applied at each node in the front elevation along the z direction.

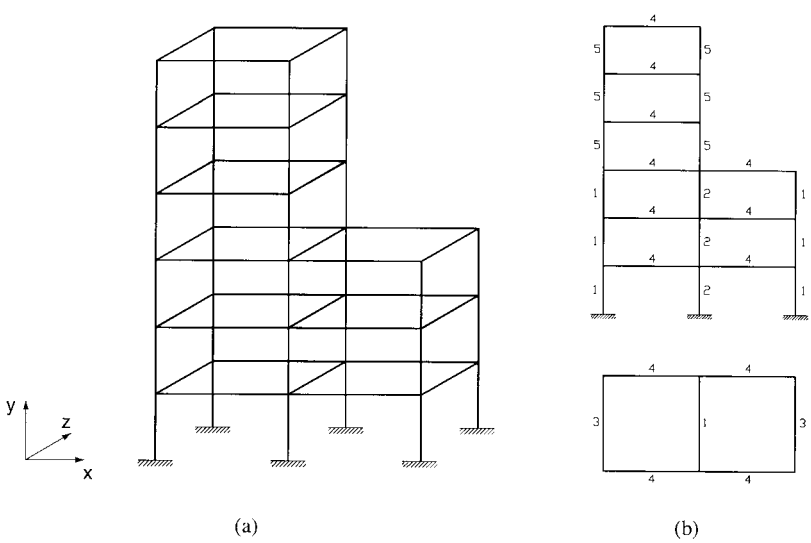

FIGURE 3 (a) Six storey space frame, (b) element groups.

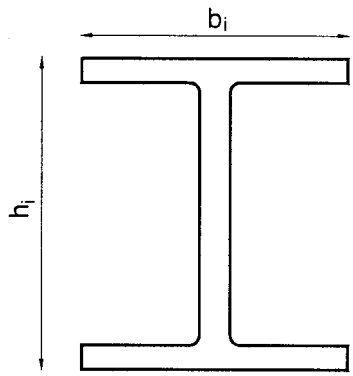

FIGURE 4 I-shape cross section.

The element members are divided into 5 groups, as shown in Figure 3(b), each one having two design variables resulting in ten total design variables. The cross section of each member is assumed to be an I-shape and for each member two design variables are considered as shown in Figure 4. The modulus of elasticity is 200 GPa and the yield stress is $\sigma_y = 250$ MPa.

The Pareto optimal set of solutions was first computed with the LWM. The performance of this method for the case of seeking the simultaneous minimization of weight and maximum displacement is depicted in Figures 5 and 6 for both static and seismic loading conditions. In Figures 5 and 6 the performance of the DFM and ESMO methods are also presented. For the case of the DFM the zero (0) point was considered as the utopian point, while four different schemes of the DFM were examined. $p = 1$: equivalent to the LWM, $p = 2$: called quadratic LWM and $p = 8$: equivalent to the $p = \infty$. The case when the weight and the first eigenperiod are considered as the objectives of the problem is depicted in Figure 7.

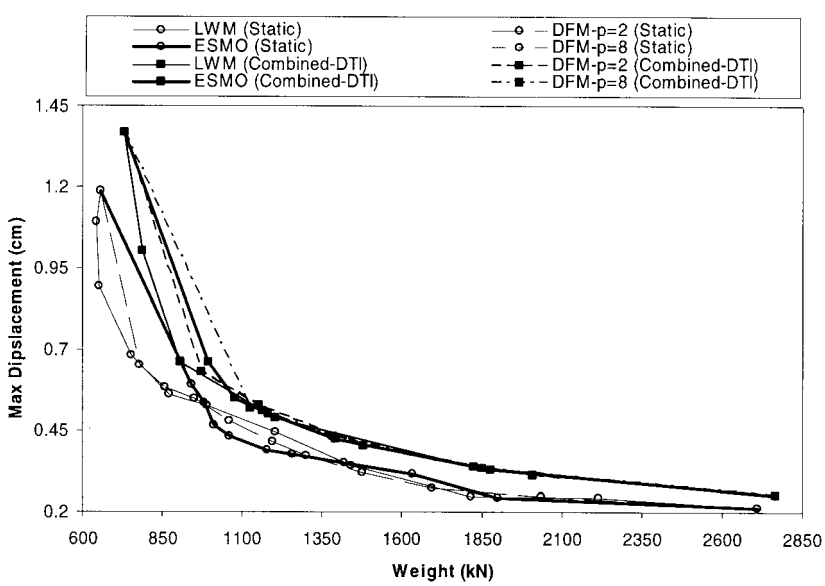

FIGURE 5 Six storey frame: performance of the methods for static and combined static and seismic loading conditions.

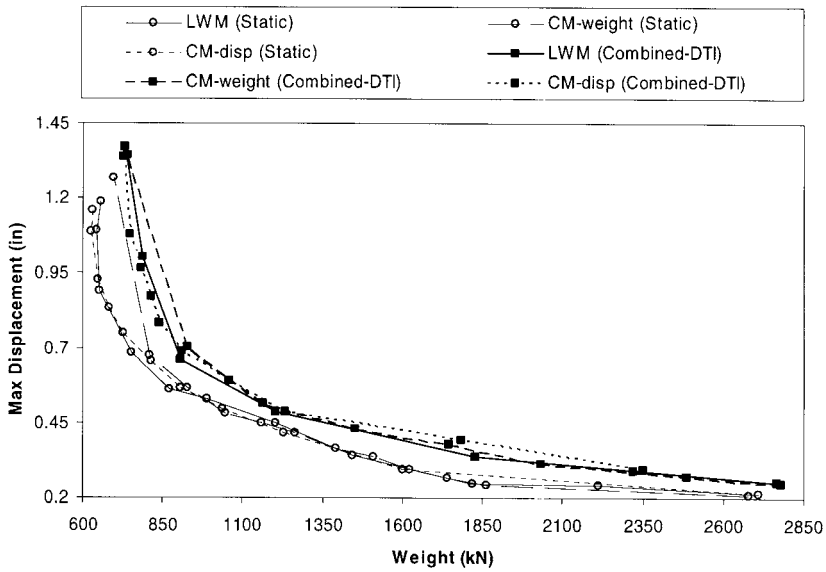

FIGURE 6 Six storey frame: performance of the methods for static and combined static and seismic loading conditions.

The CM is implemented with the following two variations: (i) The weight as the only criterion and the maximum displacement or the first eigenperiod as constraint; and (ii) the maximum displacement or the first eigenperiod as the only criterion and the weight as constraint. Figures 8 and 9 show the performance of the CM, for the simultaneous minimization of the weight and the maximum displacement. These sets of Pareto optimal solutions, are produced for the following cases: (i) different upper limits for the maximum displacement,

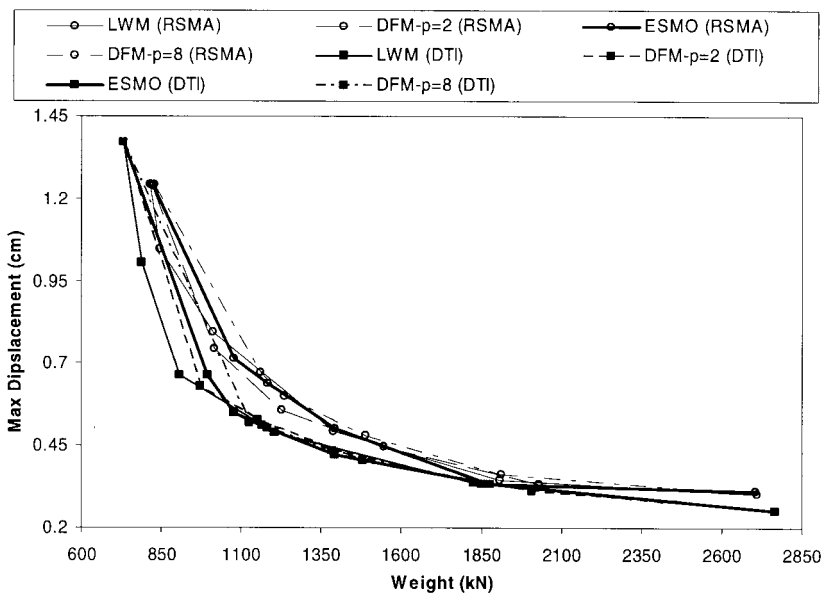

FIGURE 7 Six storey frame: performance of the methods for combined static and seismic loading conditions.

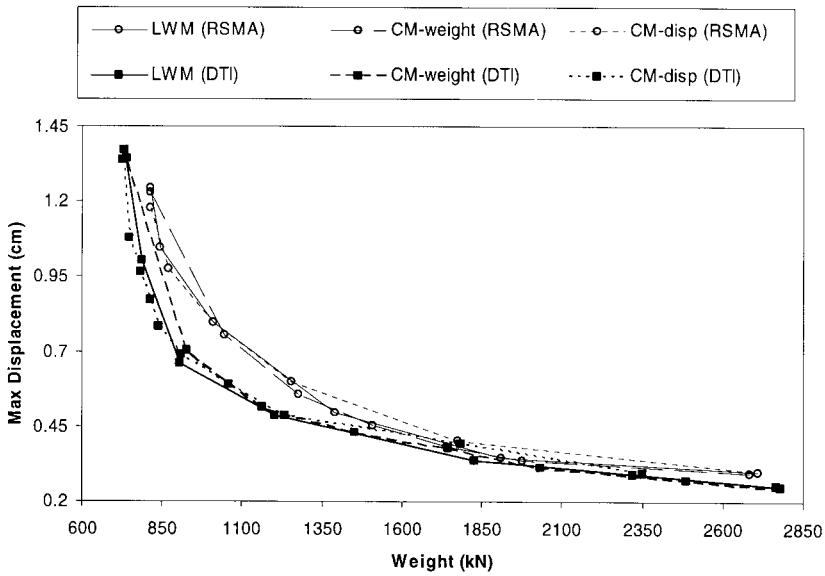

FIGURE 8 Six storey frame: performance of the methods for combined static and seismic loading conditions.

and (ii) different upper limits of the weight of the structure. Figure 10 shows the performance of the CM for the simultaneous minimization of weight and the first eigenperiod and for the cases: (i) different upper limits for the first eigenperiod, and (ii) different upper limits of the weight of the structure.

From Figures 6 and 9 it can also be seen that the Pareto optimal solutions achieved by the direct time integration approach under the multiple loading conditions of the five artificial accelerograms are lower than the corresponding designs given by the response spectrum modal analysis. Moreover, in Figures 5 and 6 and in Figures 7 and 10 it can be seen that there is little

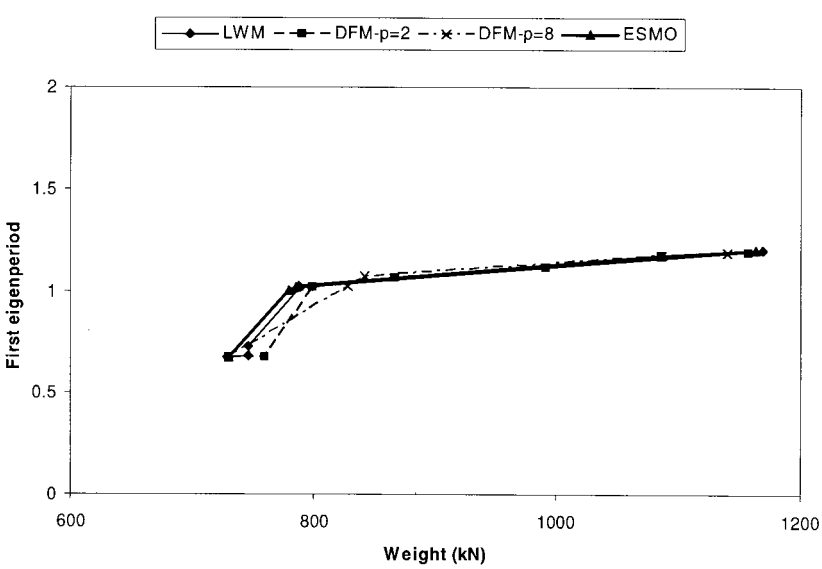

FIGURE 9 Six storey frame: performance of linear ($p = 1$), distance and ESMO methods.

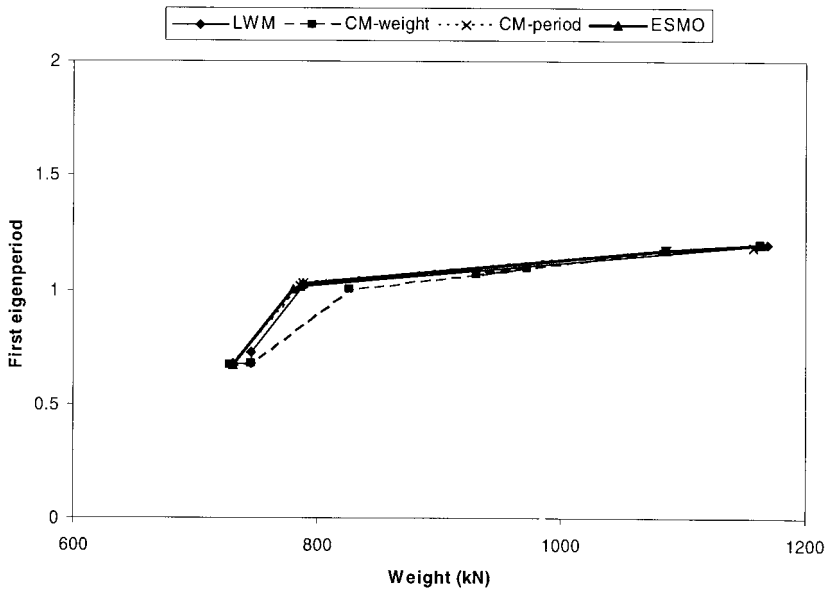

FIGURE 10 Six storey frame: performance of linear ($p = 1$), constraint and ESMO methods.

difference in the performances of the standard methods and the ESMO method, while, as can be seen from Table I, there is a substantial variation in the computing time.

6.2 Multi-layered Space Truss

The optimum design with multiple objectives of a long span three layered aircraft hangar is investigated. The objective functions considered for the problems are the weight of the structure and the maximum deflection, both of which are to be minimized. This hangar is a triple layer space truss with a 5-layered front girder spanning 130.9 m. The front girder is formed by adding two layers, one at the top and the other at the bottom of the space truss (Fig. 11). The heavily stressed top and bottom layers are designated as 'flanges' consisting of longitudinal and cross-girders, which are closed box sections. The diagonal members connecting the top and bottom flanges to the top and bottom chords of the triple-layer space frame are also closed box sections. The members of the space truss were grouped as follows: Group 1: Longitudinal members of the top and bottom flanges (Fig. 11). Group 2: Cross girders of the top and bottom flanges. Group 3: Bracing diagonals connecting the top and bottom flanges to the top and bottom chords. Group 4: Top and bottom chords of the space truss.

TABLE I Six Storey Frame: Performance of the Standard and ESMO Methods for Dealing with Multi-objectives for Dynamic Loading Conditions.

Method	*Generations*	*FE analyses*	*CPU Time (sec)*
LWM (Combined-DTI)	372	2609	254,112
ESMO (Combined-DTI)	28	367	35,788
LWM (Combined-RSMA)	411	2901	109,803
ESMO (Combined-RSMA)	31	401	15,171

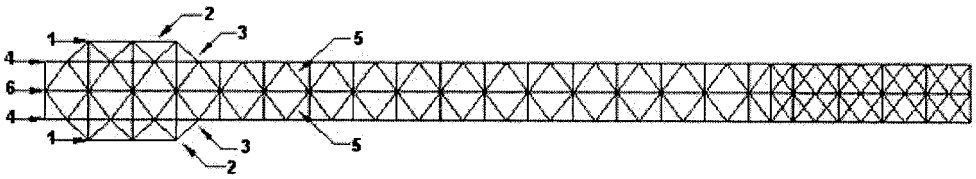

Notes:
1: Longitudinal members of the top and bottom flanges.
2: Cross girders of the top and bottom flanges.
3: Bracing diagonals connecting top and bottom flanges to top and bottom chords of the space hangar.
4: Top and bottom chords of the space hangar.
5: Diagonal bracing members connecting top and bottom chords of space hangar to middle chords.
6: Middle chords of the space hangar.

FIGURE 11 Cross-section of the space hangar. 1: Longitudinal members of the top and bottom flanges. 2: Cross girders of the top and bottom flanges. 3: Bracing diagonals connecting top and bottom flanges to top and bottom chords of the space hangar. 4: Top and bottom chords of the space hangar. 5: Diagonal bracing members connecting top and bottom chords of space hangar to middle chords. 6: Middle chords of the space hangar.

Group 5: Diagonal bracing members connecting the top and bottom chords to middle chords. Group 6: Middle chords of the space truss. The hangar comprises 3614 nodes (10,638 d.o.f.) and 12,974 members. Members of Group 1 to 3 are to be selected from the structural sections listed in Table II and members of Groups 4 to 6 from the tube sizes given in Table III. Taking advantage of the symmetry of the structure, the formulation of the problem was made for one half of the hangar depicted in Figure 12 which results in a model with 5269 d.o.f.

For this test example two cases are considered: (i) The weight as the only criterion and the maximum displacement as a constraint; and (ii) The maximum displacement as the only criterion and the weight as a constraint. The performance of the LWM for the case of the simultaneous minimization of weight and maximum displacement is depicted in Figure 13. In this figure the results of DFM with $p = 1$, 2 and 8 and ESMO methods are also presented. Figure 14 depicts the performance of the CM, for the simultaneous minimization of weight

TABLE II Properties of the Structural Members (Database 1).

Section number	*Type*	*Description*
1	ISMC 100	Single channel
2–12	2 × ISMC (75, 100, 125, 150, 175, 200, 225, 250, 300, 350, 400)	Closed box section made-up of 2 channels
13–16	2 × ISMC 400 with 2 × (8, 12, 16, 25 mm) thick MS plates	Closed box section made-up of 2 channels with 2 plates welded at top and bottom
17	4 × ISMC 400	Closed double box section made-up of 4 channels
18–22	4 × ISMC 400 with 2 × (8, 16, 20, 25, 32 mm) thick MS plates	Closed double box section made-up of 4 channels with 2 plates welded at top and bottom
23–27	4 × ISMC 400 with 4 × (20, 25, 32, 40, 50 mm) thick MS plates	Closed double box section made-up of 4 channels with 4 plates welded at top and bottom

TABLE III Properties of the Tubular Structural Members (Database 2).

Section number	*Outer diameter*	*Thickness*	*Area (mm^2)*
1	60.30	3.25	582.73
2	76.10	4.50	1012.63
3	88.90	4.85	1281.16
4	114.30	5.40	1848.19
5	139.70	5.40	2279.26
6	152.40	5.40	2494.8
7	165.10	5.40	2710.34
8	193.70	5.90	3482.35
9	219.10	5.90	3953.34
10	273.00	5.90	4952.8

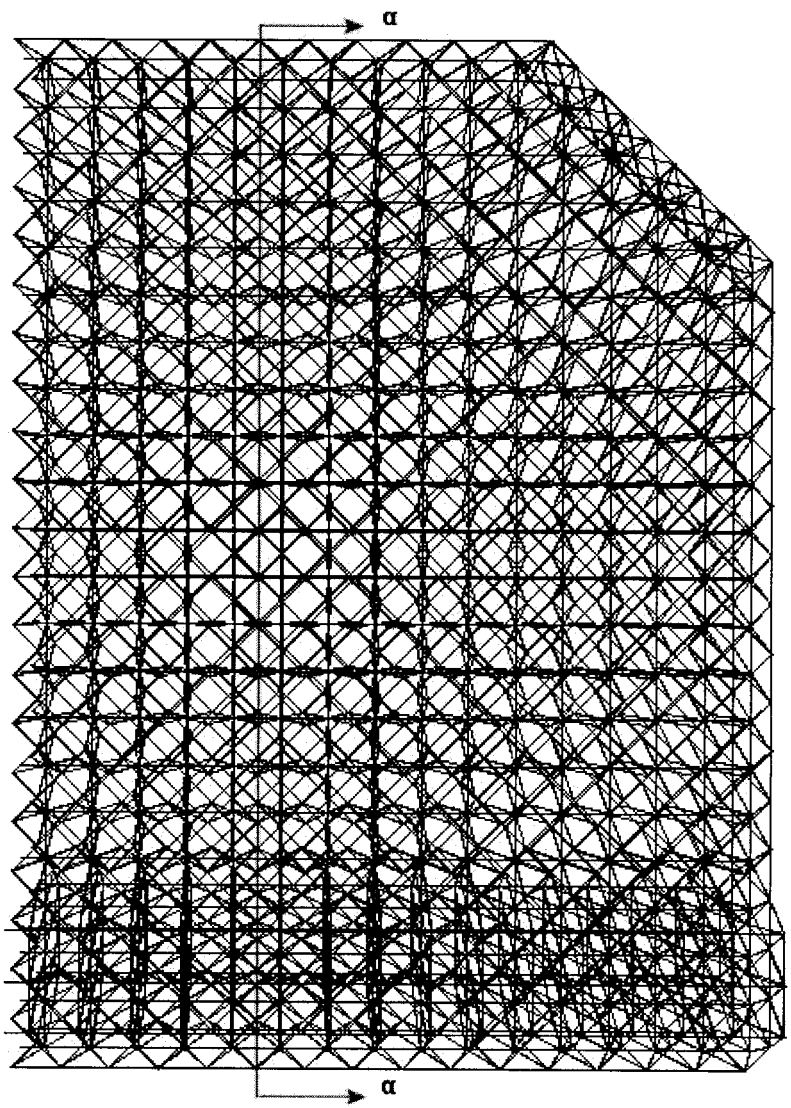

FIGURE 12 Multi-layered space truss.

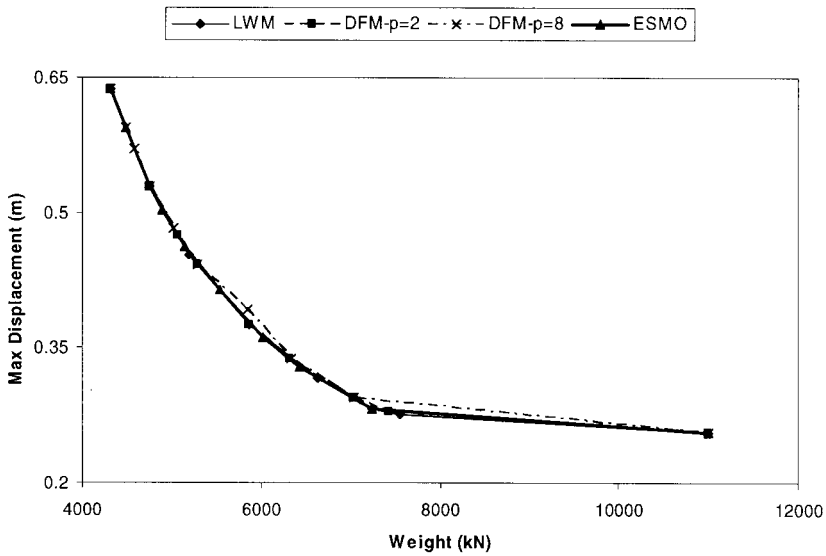

FIGURE 13 Multi-layered space truss: performance of linear, distance and ESMO methods.

and maximum displacement. These sets of Pareto optimal solutions, are produced for different upper limits for the maximum displacement and for different upper limits of the weight of the structure. In Figures 13 and 14 it can be seen that there is little difference in the results obtained by the standard methods and the ESMO method while, as can be seen from Table IV, there is a substantial improvement in the computing time with the proposed implementation.

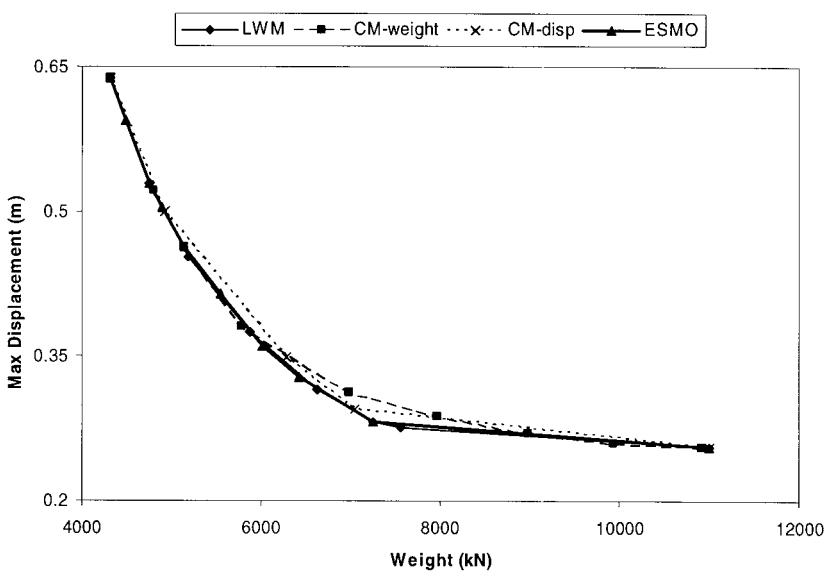

FIGURE 14 Multi-layered space truss: performance of linear, constraint and ESMO methods.

TABLE IV Multi-layered Space Truss: Performance of the Standard and ESMO Methods for Dealing with Multi-objectives.

Method	*Generations*	*FE analyses*	*CPU Time (sec)*
LWM	195	1163	7917
ESMO	28	312	2119

7 CONCLUSIONS

Evolution Strategies can be considered as an efficient tool for multi-objective design optimization of structural problems such as space frames and multi-layered space trusses under static and seismic loading conditions. The proposed modified evolution strategies method for treating multi-objective optimization problems proved to be a robust and reliable optimization tool giving almost identical results compared to those obtained by the standard methods used in the past such as the linear weighting, distance function and constraint methods.

In terms of computational efficiency it appears that all three standard methods considered require similar computational effort with approximately the same number of generation steps. On the other hand, the proposed method requires almost one order of magnitude less computing time than the standard methods. The presented results show that it is possible to achieve an optimal design under seismic loading and multiple objectives. Both design methodologies based on a number of artificially generated earthquakes and the response spectrum modal analysis adopted by the seismic codes have been implemented and compared. The dynamic approach based on time history analyses gives more economic designs than the approximate response spectrum modal analysis, at the expense of requiring more computational effort.

References

[1] Zeleny, M. (1982). *Multiple Criteria Decision Making.* McGraw-Hill, New York.
[2] Haimes, Y. Y. and Hall, W. A. (1974). Multi-objectives in water resource systems analysis: The surrogate worth trade off method. *Water Resources Res.*, **10**, 615–624.
[3] Cohon, J. L. (1978). *Multi-objective Programming and Planning.* Academic Press, New York.
[4] Fonseca, C. M. and Fleming, P. J. (1995). An overview of evolutionary algorithms in multi-objective optimization. *Evolutionary Computations*, **3**(1), 1–16.
[5] Papadrakakis, M., Lagaros, N. D. and Plevris, V. (2001). Optimum design of space frames under seismic loading. *International Journal of Structural Stability and Dynamics*, **1**(1), 105–124.
[6] Johnson, E. H. (1976). Disjoint design spaces in optimization of harmonically excited structures. *AIAA Journal*, **14**(2), 259–261.
[7] Eurocode 1, Actions on structures. (1991). Part 1.1: Densities, self-weight and imposed loads for buildings, Part 1.3: Snow loads, Part 1.4: Wind loads, EN 1991-1-1/EN 1991-1-3/EN 1991-1-4.
[8] Eurocode 3, Design of steel structures. (1993). Part 1.1: General rules, Part 1.5: Strength and stability of planar plated structures without transverse loading, EN 1993-1-1/EN 1993-1-5.
[9] Pareto, V. (1896–1897). *Cours d' économique politique*, Vol. 1&2. Rouge, Lausanne.
[10] Adali, S. (1983). Pareto optimal design of beams subjected to support motion. *Computers and Structures*, **16**, 297–303.
[11] Hajela, P. and Shih, C. J. (1990). Multi-objective optimum design in mixed integer and discrete design variable problems. *AIAA Journal*, **28**(4), 670–675.
[12] Rozvany, G. I. N. (1989). *Structural Design via Optimality Criteria*. Kluwer, Dordecht.
[13] Koski, J. (1984). Bicriterion optimum design method for elastic trusses. Acta Polytechnica Scandinavica, Mechanical Engineering Series No 86, *Dissertation*, Helsinki.
[14] Sandgren, E. (1984). Multicriteria design optimization by goal programming. In: Adeli, H. (Ed.), *Advances in Design Optimization*. Chapman & Hall, pp. 225–265.
[15] Kamal, C. S. and Adeli, H. (2000). Fuzzy discrete multicriteria cost optimization of steel structures. *Journal of Structural Engineering*, **126**(11), 1339–1347.

[16] Coello, C. A. and Christiansen, A. D. (2000). Multi-objective optimization of trusses using genetic algorithms. *Computers and Structures*, **75**, 647–660.
[17] Koski, J. (1994). Multicriterion structural optimization. In: Adeli, H. (Ed.), *Advances in Design Optimization*. Chapman & Hall, pp. 194–224.
[18] Schaffer, J. D. (1984). Multiple objective optimization with vector evaluated genetic algorithms. *PhD thesis*, Vanderbilt University.
[19] Fonseca, C. M. and Fleming, P. J. (1993). Genetic algorithms for multiobjective optimization: Formulation, discussion and generalization. In: Forrest, S. (Ed.), *Proceedings of the 5th International Conference on Genetic Algorithms*. Morgan Kaufmann, San Mateo, California, pp. 416–423.
[20] Horn, J., Nafpliotis, N. and Goldberg, D. E. (1994). A niched Pareto genetic algorithm for multiobjective optimization. In *Proceedings of the 1st IEEE Conference on Evolutionary Computation*, Vol. 1. IEEE World Congress on Evolutionary Computation, IEEE, Piscataway, NJ, pp. 82–87.
[21] Zitzler, E. (1999). Evolutionary algorithms for multiobjective optimization: Methods and applications. *PhD Thesis*, Swiss Federal Institute of Technology Zurich, Computer Engineering and Networks Laboratory.
[22] Taylor, C. A. (1989). EQSIM, A program for generating spectrum compatible earthquake ground acceleration time histories. Reference Manual. Bristol Earthquake Engineering Data Acquisition and Processing System.
[23] Papadrakakis, M., Tsompanakis, Y. and Lagaros, N. D. (1999). Structural shape optimization using evolution strategies. *Engineering Optimization*, **31**, 515–540.
[24] Papadrakakis, M., Lagaros, N. D. and Tsompanakis, Y. (1998). Structural optimization using evolution strategies and neural networks. *Comp. Meth. Appl. Mechanics and Engrg.*, **156**, 309–333.
[25] Schwefel, H. P. (1981). *Numerical Optimization for Computer Models*. Wiley & Sons, Chichester, UK.
[26] Thierauf, G. and Cai, J. (1996). Structural optimization based on evolution strategy. In: Papadrakakis, M. and Bugeda, G. (Eds.), *Advanced Computational Methods in Structural Mechanics*. CIMNE, Barcelona, pp. 266–280.